
Molecular Crystals and Liquid Crystals

Publication details, including instructions for authors and subscription information:
http://www.tandfonline.com/loi/gmcl20

# Mesoscopic Concentration Variations Analyzed by Secondary Ion Mass Spectrometry

Charlotte B. K. Kjellander [a] , Leo J. van Ijzendoorn [b] , Arthur M. de Jong [b] , Dirk J. Broer [c] & Hans J. W. Niemantsverdriet [d]

[a] Cyclotron Laboratory, Department of Applied Physics, Eindhoven University of Technology, Eindhoven and Dutch Polymer Institute (DPI), Eindhoven

[b] Cyclotron Laboratory, Department of Applied Physics, Eindhoven University of Technology, Eindhoven

[c] Laboratory of Polymer Technology, Department of Chemical Engineering, Eindhoven University of Technology, Eindhoven

[d] Laboratory of Inorganic Chemistry and Catalysis, Department of Chemical Engineering, Eindhoven University of Technology, Eindhoven

Version of record first published: 31 Jan 2007

*Mol. Cryst. Liq. Cryst.*, Vol. 434, pp. 171/[499]–182/[510], 2005

ISSN: 1542-1406 print/1563-5287 online
DOI: 10.1080/15421400590955613

Taylor & Francis
Taylor & Francis Group



# Mesoscopic Concentration Variations Analyzed by Secondary Ion Mass Spectrometry

**Charlotte B. K. Kjellander**
Cyclotron Laboratory, Department of Applied Physics, Eindhoven University of Technology, Eindhoven and Dutch Polymer Institute (DPI), Eindhoven

**Leo J. van Ijzendoorn**
**Arthur M. de Jong**
Cyclotron Laboratory, Department of Applied Physics, Eindhoven University of Technology, Eindhoven

**Dirk J. Broer**
Laboratory of Polymer Technology, Department of Chemical Engineering, Eindhoven University of Technology, Eindhoven

**Hans J. W. Niemantsverdriet**
Laboratory of Inorganic Chemistry and Catalysis, Department of Chemical Engineering, Eindhoven University of Technology, Eindhoven

*Secondary ion mass spectrometry (SIMS) was used to identify concentration gradients of polyacrylate samples. Applying discriminant function analysis (DFA) on the SIMS spectra resulted in visualized separations between different sample concentrations. We identified and separated concentrations of polyacrylate blends; from the separation we can construct calibration curves. The visual identification was followed in depth of a poly(fluoro-acrylate) film covered by poly(isobornylmethacrylate), which served as model sample of a photo-induced phase separated device. The combination of SIMS and DFA offers new possibilities to study the phase separation processes. Furthermore, it can predict how the phase separation creates mesoscopic layered electro-optical devices.*

**Keywords:** concentration gradient; discriminant function analysis; multivariate statistics; phase separation; polymer dispersed liquid crystals; secondary ion mass spectrometry

The work was granted by the Dutch Polymer Institute (NL), in project: DPI 277.

Address correspondence to Charlotte B. K. Kjellander, Cyclotron Laboratory, Department of Applied Physics, Eindhoven University of Technology, P.O. Box 513, NL-5600MB Eindhoven. E-mail: b.k.c.kjellander@tue.nl

## INTRODUCTION

Photo-induced phase separation during polymerization of a homogeneous blend of polyfunctional monomers and liquid crystals (LCs) creates a polymer network with domains of LCs. LCs are of interest for the electro-optical industry since they possess a high degree of order while still liquid, as well as being birefringent. The latter results in varied refractive indices when external fields switch the direction of the LC molecules. Switchable devices can be made where the polymer network is used as a support, without losing the characteristic properties of the LCs, and the refractive index of the LC is modulated by an external electrical field. Examples of such devices are polymer dispersed liquid crystal (PDLC) films, where domains of LC are embedded in a polymer network [1]. The optical effects of PDLC films depend on the birefringence and density of the LCs in the polymer network.

During the phase separation process, a variation in light intensity will result in a variation of LC concentration in the polymer matrix. Masked lithography and laser beam holography alter the light intensity and thus the composition in the sample on lateral scale, and in the case of holography even in depth [2,3]. As a result the PDLC becomes structured such that for instance a switchable reflective grating is being formed. Alternatively, stratified LC-polymer films can be achieved with ordinary UV-light source where an intensity gradient over the cross-section of the film is created due to light-absorption of molecules in the curing mixture. The result is a complete phase separation of a polymer and a liquid crystalline phase separated by a well-defined layer structure [4,5].

Similarly, polymer films with concentration gradients of two (or more) polymerizable components have been made by means of photo-induced phase separation processes. One example is: devices to increase the viewing angle for e.g., LCD screens; mixtures of two acrylates were polymerized through a mask to create a distribution of refractive indices in the film [6].

Controlling photo-induced phase separation to produce the desired concentration gradients of LCs in more complex structured PDLC films remains difficult. One major reason is that we have no satisfactory way to accurately identify when and where the phase separation takes place. Experimentally, imaging techniques such as spectroscopy and scanning electron microscopy usually characterize the devices in respect of reflected/transmitted wavelength and grating periodicity. However, these analysis techniques are dependent on the contrast between the layers. This reduces their accuracy at determining compositions of layers with similar transmittance and morphology.

An analysis technique that identifies phase separation on the molecular level would aid in our development of structured PDLC films.

Secondary ion mass spectrometry (SIMS) provides information at the molecular scale and offers the possibility to determine LC concentrations in PDLC films. The SIMS technique analyzes secondary ions sputtered from a surface. The secondary ions are detected as charged mass fragments (m/z) of the sample material, and the unique correlations between the intensities of the sputtered mass fragments identify the sample material. SIMS can be applied in two modes: static and dynamic. Static SIMS uses low primary ion doses to sputter large mass fragments from the sample surface [7]. Dynamic SIMS uses higher primary ion doses and charged mass fragments are followed in depth, yielding depth profiles of the samples.

Traditionally, dynamic SIMS has been applied to analyze trace elements in depth of inorganic materials [8]. For organic materials, focus has mainly been concentrated on static SIMS to identify large molecules, as e.g. proteins [9], or specific polymer end-groups at the surface, as e.g. different butyl end groups at the surface of polystyrene [10].

Furthermore, the use of dynamic SIMS on organic materials is less explored due to the complex fragmentation/ionization processes caused by the higher primary ion dose necessary to sputter through the sample. SIMS depth profiling of polymers is generally applied to labeled polymer layers, e.g. to study the self-stratification depth of different polystyrene mixtures labeled by deuterium and bromine [11].

Recently, van Gennip applied the multivariate statistical method discriminant function analysis (DFA) on dynamic SIMS spectra to obtain concentrations of organic solar cell materials [12]. Similarly, we presented a method to derive concentrations of un-labeled PDLC samples [13]. Since DFA creates functions, which maximize the difference between a priori selected groups in a set of SIMS spectra, DFA is particular suited to identify groups with similar chemical compositions such as in layers of multi-layered PDLC devices.

In our above-mentioned study however, we had quantification problems due to evaporation of the nematic LC molecules. Therefore, the purpose of this study was to use dynamic SIMS and DFA to identify concentration variations of layered polyacrylate samples, where the LC molecules were polymerizable, and thus did not evaporate during analysis. We analyzed several samples of poly(LC-acrylates) and poly(acrylates). From the analysis we derived calibration curves. We made SIMS depth profiles of a two-layered sample, and with DFA we employed our method to identify concentration gradients in the layers.

## METHODS

We studied the following monomers: a cyanobiphenyl hexyloxy acrylate (LC6A) synthesized at Philips Research (Eindhoven, NL); phenylacrylate (PhA, Polyscience Inc.); iso-bornylmethacrylate (iBMA, Aldrich); and 1H1H6H6H perfluoro-1,6-hexyldiacrylate (F-acrylate, Exfluor) (Fig. 1).

Polymer films were prepared by spin-coating monomers on silicon wafers followed by UV-curing (Philips PL-S 9W/10 at 365 nm and 3 mW/cm$^2$) at room temperature in a nitrogen environment. One weight% of the photo-initiator Irgacure 651 (Ciba) was added to the monomers to start the polymerization. We calibrated the spin-coater by measuring film thicknesses of the polymerized PhA monomers with a Tencor P-10 profilometer. Polymer films were prepared from PhA or iBMA monomers only, as well as from blends with 13 wt% LC6A in PhA and 52 wt% LC6A in PhA.

The polymer films of LC6A monomer were prepared differently. Since the monomer LC6A is crystalline at room temperature it needs an elevated temperature or solvent, to be processed. We chose to doctor blade the monomer to a thickness of 1 μm, at 80°C onto Si-wafers. Similarly, a film was prepared of a blend with 39 wt% LC6A in iBMA. The polymerizations were done at 80°C.

Furthermore, a two-layered sample was prepared in two steps. Monomer mixture of pure F-acrylate was applied in a 1 μm spaced glass cell and polymerized at room temperature. Then, the top glass-plate was removed, and on top of the poly(F-acrylate) film iBMA was spin-coated. The iBMA monomers were cured by UV-light at room

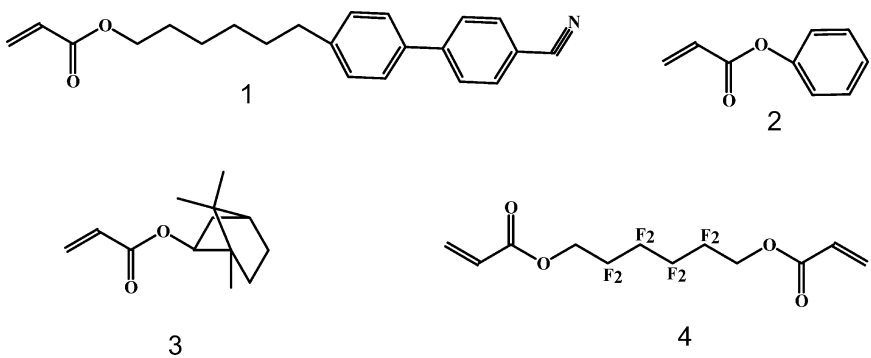


**FIGURE 1** The monomers used in this study: **1** liquid crystalline monoacrylate (LC6A), **2** phenylacrylate (PhA), **3** iso-bornylacrylate (iBMA), and **4** 1H1H6H6H perfluoro1,6-hexyldiacrylate (F-acrylate).

temperature and in $N_2$ environment. The thickness of the top poly(iBMA) coating was estimated to be 20–40 nm according to the thickness calibration.

All dynamic SIMS measurements were obtained on a VG Ionex SIMS system, equipped with a liquid metal ion source, MIG 102, and a M12-2 s (< 800 amu) quadrupole mass analyzer which measured ten negatively charged mass fragments in consecutive order during constant sputtering. The time for measuring each of the m/z ratios once is called a cycle. The mass spectra were obtained by scanning the quadrupole over a range of m/z ratios during continuous sputtering. The primary ion source was operated with 10 keV and 4.2 nA $Ga^+$, and scanned over an area of $200 \times 200\,\mu m$. The secondary ion yield was, with the help of an electronic gate, obtained from the centered 10% of the total sputtered area. In the case of measuring mass spectra, no electronic gating was used.

Furthermore, to prevent charging of the samples during analysis we used a LEG 31 F electron flood gun and covered samples with a monolayer conducting metal. The sputtered depth of the two-layered sample was measured by an optical profilometer (Fogale Zoomsurf 3D) to convert the measured cycles to depth units. The sputter speed was assumed to be constant through depth.

SIMS spectra were analyzed with the multivariate statistical method DFA. This analysis results in a number of functions that maximize the difference between a priori selected groups in a set of SIMS spectra [14]. A DFA function consists of a linear combination of the number of counts per m/z ratio weighted by coefficients. The degrees of freedom for the discriminant function analysis, which determines the number of independent DFA functions, are dependent on the number of a priori selected groups.

To determine whether one or more DFA function significantly can display the differences between the groups, the chi-square distributions of the DFA functions are compared to the significance level [14,15]. A low level of significance reveals a high probability that the function represents a unique combination of variables corresponding to a non-specific sample property, which can be distinguished. The amount of variance captured by the functions shows how much of the initial information the DFA functions display.

By plotting two significantly different functions with the largest variance, the samples are represented by points in the plane of the functions. If the samples have unique values of the DFA functions and enough variance is captured by the two functions; the correlation between the m/z ratios explained by the two functions can distinguish between samples. Consequently, the samples will appear on a curved

line in the plane in consecutive order of the concentration. With known concentration of the samples, DFA allows to construct a calibration curve from which unknown concentrations can be identified.

We minimized the influences on the DFA analysis of variations in measuring conditions by normalizing the dynamic SIMS spectra on total intensity per depth unit. The normalization was done for all samples.

We used the commercial software package SPSS (release 11.0.1, SPSS Inc.) for calculating the discriminant function values.



## RESULTS

The dynamic SIMS mass spectra of polymerized LC6A (poly(LC6A), Fig. 2a) showed low-mass fragment ions coming from six major m/z ratios: 12, 16, 24–25, and 48. All of these m/z ratios originate from common (non-specific) carbohydrate ion fragments, except m/z 16 that represents $O^-$. The measured mass intensities of poly(PhA) also showed low mass fragments from common hydrocarbon ions (figure 2b), with the exceptions of the ratio m/z 16: $O^-$, and the ratio m/z 19 ($F^-$). The latter ion, $F^-$, we considered as contamination, since no fluorine should be present in the PhA polymer. The correlations between the intensities of the m/z ratios were not equal for the two samples in Figure 2. The mass spectra from the poly(iBMA) (Fig. 3) only showed common hydrocarbon mass-fragments.

Eventhough none of the measured m/z ratios was specifically characteristic for any of the three polymers (poly(LC6A), poly(PhA)

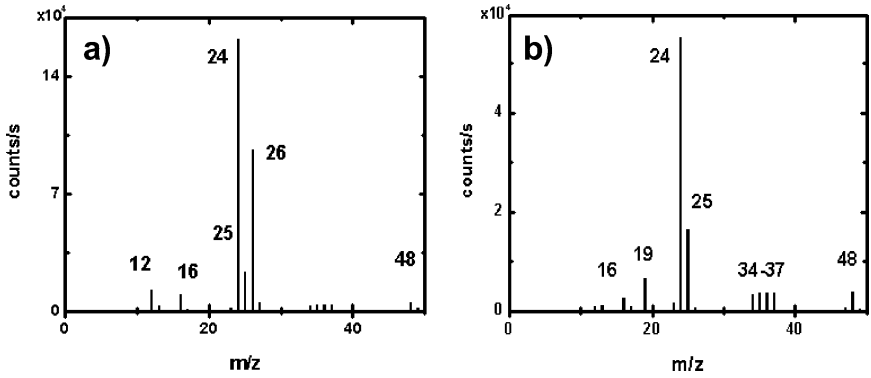


**FIGURE 2** Dynamic SIMS mass spectra of two polyacrylate films: a) poly (LC6A) and b) poly(PhA). The most intense mass fragments are noted in the spectra.

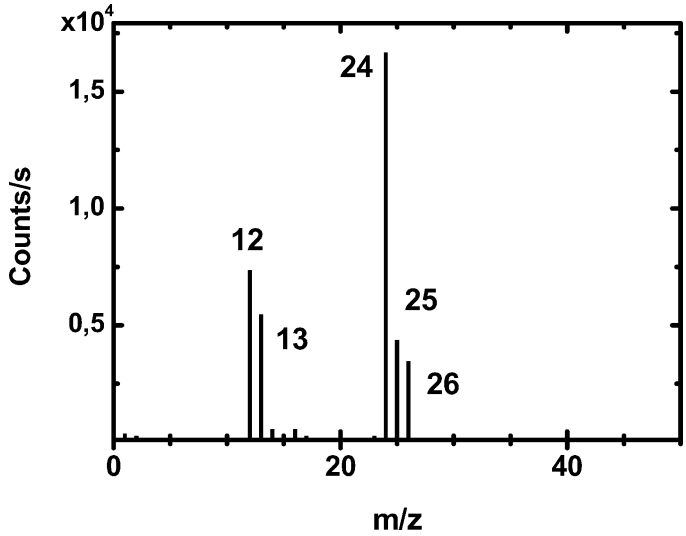


**FIGURE 3** Dynamic SIMS mass spectrum of poly(iBMA). The most intense mass fragments are shown in the spectrum.

and poly(iBMA)), the fingerprints (the combinations of the m/z ratios for each individual compound that were measured in the SIMS mass spectra) are unique for the three different materials. Applying DFA on the dynamic SIMS data can mathematically identify the differences between the polymers.

First, we analyzed the SIMS mass spectra of four polymer films of poly(LC6A), poly(PhA) and two polymerized blends of LC6A and PhA. We used seven common mass fragments (m/z 12, 16, 24–26 and 48) for the DFA analysis. These m/z ratios were chosen based on the mass spectra of poly(LC6A) and poly(PhA) (Fig 2). The four polymer samples were defined as one group each in the DFA analysis; this gave three degrees of freedom for the analysis. As a consequence, three DFA functions are allowed. The two first functions were significant different below the 5% level, while the third was significantly different below the 15% level. The first two functions captured 99,7% of the variance. Since the two first DFA functions were significantly different and captured large amount of variance, we used these two in the DFA plot (Fig. 4). In the plot the different compositions of the films were separated, as a consequence of dissimilar DFA values. The increasing concentration of PhA of the samples is visualized in Figure 4. The arrow in the DFA plot, indicating a calibration curve, follows the increase of concentration.

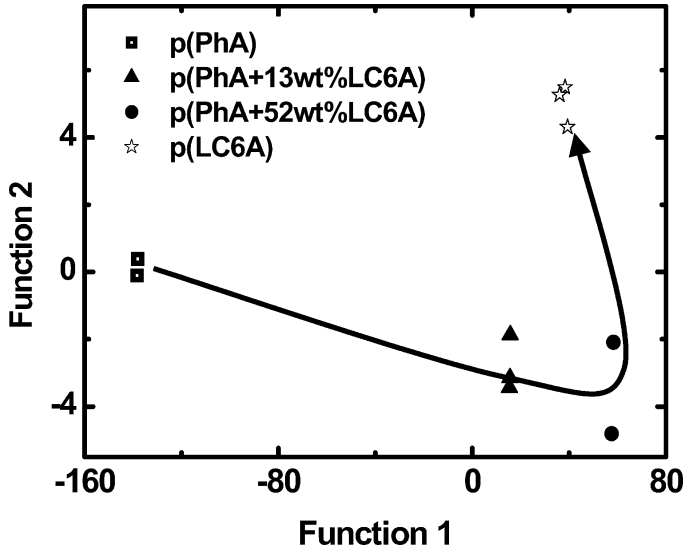


**FIGURE 4** Discriminant function analysis (DFA) of poly(LC6A), poly(PhA), and two polymerized blends of LC6A and PhA. DFA creates independent functions from the SIMS spectra, with these functions DFA discriminates between the compositions in the samples. Function 1 and 2 explain significant difference between the sample compositions (at a significance level of 5%) and the functions contains 99.7% of the initial data from the SIMS spectra. As a result, the increasing concentration of LC6A in the samples is followed by the arrow in the plot.

Next we studied the samples of poly(LC6A), poly(iBMA), and a polymerized blend of LC6A and iBMA. The dynamic SIMS spectra from these samples were obtained by following ten m/z ratios in depth. Of the ten mass fragments analyzed, we used four common ones (m/z 24–26 and 48) for the DFA. The four mass fragments chosen were detectable in all samples and gave stable intensities during the in-depth measurement. Each sample was divided into three groups, where every group consisted of 20 SIMS measuring cycles. In total we pre-defined 9 groups for the DFA analysis. The purpose was to investigate whether DFA could cluster the groups from the same samples as well as separate between the samples with different compositions.

The DFA analysis of the three samples, which in total consisted of 9 groups, allows 8 degrees of freedom. Out of the 8 DFA functions, the two first functions had 99.5% of variance and they were both significantly different on the 0.01% level. When plotting these functions (Fig. 5), we found the groups from the same samples clustered while the different sample compositions were separated.

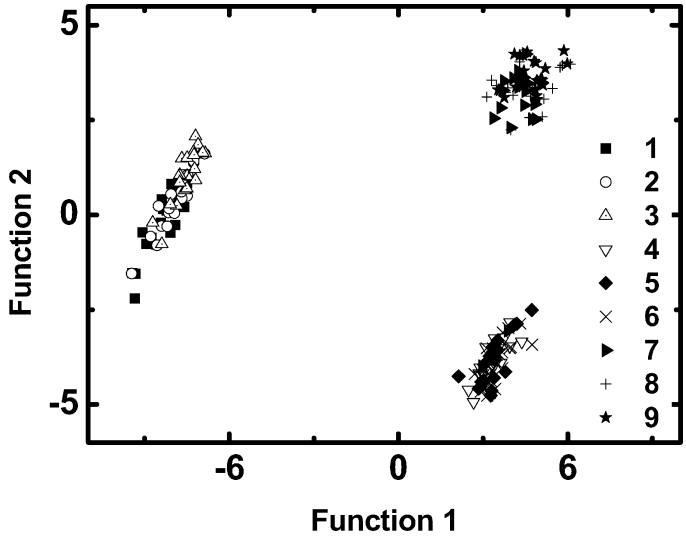


**FIGURE 5** The two first DFA functions plotted for poly(LC6A), poly(iBMA), and a polymerized blend of LC6A and iBMA. The samples were divided into three groups each, where group 1–3 corresponded to poly(iBMA), group 4–6 to the blend, and group 7–9 to poly(LC6A).

Finally, we analyzed the sample of poly(F-acrylate) covered by poly(iBMA). The SIMS depth profile of this sample followed ten mass fragments in depth (m/z 12, 13, 16, 19, 24–26, 31, 38, and 48) (Fig. 6). The depth of the sputtered crater measured 101 nm, and since we assume the sputter speed to be constant, each cycle (measuring the ten masses) corresponds to 1 nm. In the SIMS spectra, the intensity of m/z 19 ($F^-$) detected specifically poly(F-acrylate). Surprisingly, we detected m/z 19 at the top of the sample, where no fluorine-containing polymer should be present. Furthermore, the intensity of m/z 19 gradually increased to a constant value, which was approached at the depth of approximately 60 nm.

Since the m/z ratio 19 labeled the poly(F-acrylate), this mass fragment could alone identify the pure poly(F-acrylate) film. We studied the possibility to identify the films by analyzing non-specific mass fragments by applying DFA on the depth profile of the two-layered sample together with dynamic SIMS spectra of poly(iBMA) and poly(F-acrylate). The DFA analysis was performed using four common mass fragments (m/z 24–26 and 48). The depth profile was divided into five groups, where each group consisted of a depth interval of 20 nm (20 cycles). In total we pre-defined seven groups, which lead

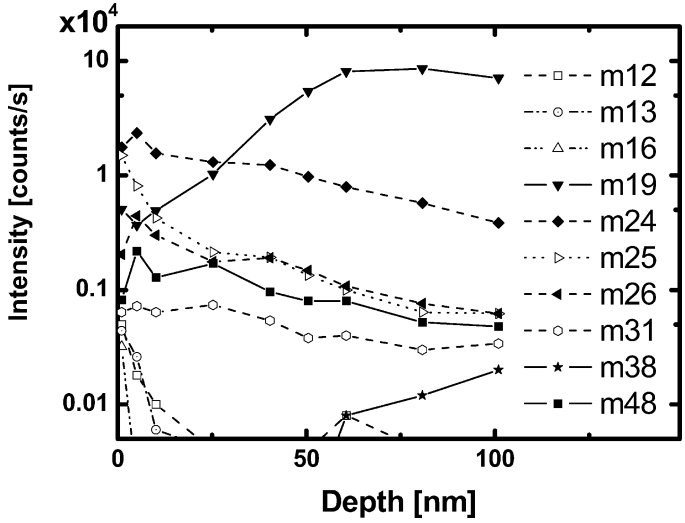


**FIGURE 6** Dynamic SIMS depth profile of the poly(F-acrylate) film covered by poly(iBMA).

to six degrees of freedom and maximum six DFA functions. From the analysis, the three first DFA functions were significant different at a level 0.01%, and the two first functions captured together 99.4% of the variance. The plot of function 1 versus function 2 separated the pure poly(iBMA) and poly(F-acrylate) samples, and spread the data points of the groups from the depth profile between them (Fig. 7). We found that group 4 and 5 coincided with the cloud of points belonging to the poly(F-acrylate). This showed that the pure poly(F-acrylate) layer in the depth profile started at around 60 nm, which was also seen from the labeled SIMS spectra. Note that the first group did not fall on the poly(iBMA) in Figure 7. The separation between group 1 and poly (iBMA) shows that the top-coating on the two-layered sample was not pure poly(iBMA). This is in agreement with the SIMS depth profile of m/z 19.

## DISCUSSION

In this study we identified different concentrations of polyacrylates by dynamic SIMS and DFA, which generated calibration curves. We showed how DFA followed concentrations in depth of a two-layered polyacrylate sample.

We demonstrated that two DFA functions identified four different sample compositions (Fig. 4). Also, two DFA functions clustered

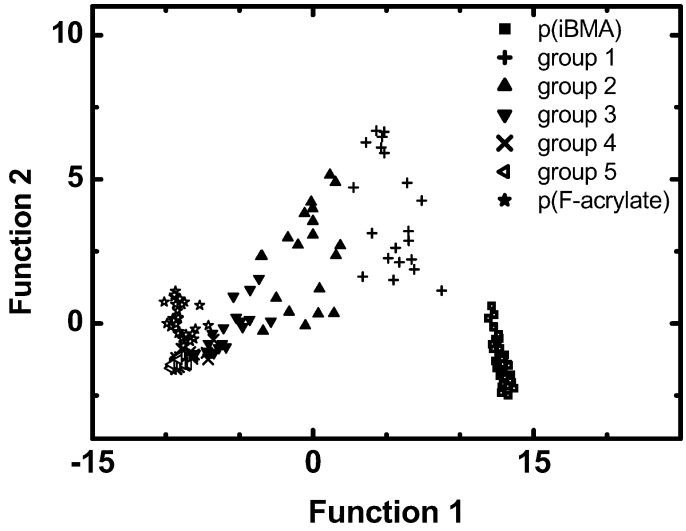


**FIGURE 7** DFA of poly(iBMA), poly(F-acrylate) and sample in Figure 4, which was divided into 5 groups, where group 1 contained the first 20 nm from the SIMS depth profile, the second group the following 20 nm, etc.

groups of measurements from the same sample (as in Fig. 5). This visual identification is useful to recognize concentrations (in the form of a calibration curve), and to identify layer compositions in layered samples such as electro-optical gratings.

The accuracy of the calibration curves depends on the spread of data points of the same samples in the DFA plot. We investigated possible sources of these variations and found that the scattering of the data points in the DFA plot correlated with instabilities of the SIMS yields. The instabilities in the SIMS yields might depend on local concentration variations in the samples, local charging of the sample during SIMS analysis, or other effects, which are not easy to identify. Variations of the concentrations on a scale comparable to, or larger than, the analyzed volume might be a source for instabilities. Note that we implicitly assumed that local variations, if any, were on a smaller scale than the analyzed volume.

As a comparison with optical devices, which can be prepared by e.g. holography, the sample of poly(F-acrylate) covered by poly(iBMA) served as a model for one pitch in a layered grating. When layered electro-optical devices are produced by photo-induced phase separation, the interfaces depend on the light intensity profile curing the film, and the interfaces are unlikely to be sharp. The interface of

our model sample showed a similar behavior; from the top of the sample the intensities of the m/z ratios gradually changed until a depth of about 60 nm was reached. From this depth on, the intensities remained stable, and we assumed to have reached the poly(F-acrylate) film at 60 nm. Apparently the iBMA monomers migrated into the F-acrylate polymer before polymerizing, and resulted in a model for samples with a concentration gradient.

To conclude: our method combines dynamic SIMS with DFA to identify variations in chemical composition. As a result, concentration gradients can be followed in mesoscopic depth intervals. The method offers new possibilities to measure layer compositions created by photo-induced phase separation processes. This will, in turn, help us to predict how these processes create layered electro-optical devices.



## REFERENCES

[1] Doane, J. W., Vaz, N. A., Wu, B.-G., & Žumer, S. (1986). *Appl. Phys. Lett.*, *48*, 269.
[2] Sutherland, R. L., Tondigalia, V. P., Natarajan, L. V., Bunning, T. J., & Adams, W. W. (1994). *Appl. Phys. Lett.*, *64*, 1074.
[3] Escuti, M. J. & Crawford, G. P. (2002). *Mater. Res. Soc. Symp. Proc.*, *709*, 293.
[4] Penterman, R., Klink, S. I., Koning, H. de, Nisato, G., & Broer, D. J. (2002). *Nature*, *417*, 55.
[5] Vorflusev, V. & Kumar, S. (1999). *Science*, *283*, 1903.
[6] Leewis, C. M. (2003). *Formation of Mesoscopic Polymer Structures for Optical Devices, a Nuclear Microprobe Study*, chapt 6, Universiteitsdrukkerij Technische Universiteit Eindhoven, Eindhoven, NL, 125.
[7] Davies, N., Weibel, D. E., Blenkinsopp, P., Lockeyer, N., Hill, R., & Vickerman, J. C. (2002). *Appl. Surf. Science.*, *9240*, 1.
[8] Siemensen, C. J. & Södervall, U. (2000). *Surf. Interface Anal.*, *30*, 309.
[9] Wagner, M. S., Horbett, T. A., & Castner, D. G. (2003). *Langmuir*, *19*, 1708.
[10] Vanden Eynde, X. & Bertrand, P. (1997). *Surf. Interface Anal.*, *25*, 878.
[11] Rysz, J., Ermer, H., Budkowski, A., Lekka, M., Bernasik, A., Wróbel, S., Brenn, R., Lekki, J., & Jedliński, J. (1999). *Vacuum.*, *54*, 303.
[12] Gennip, W. J. H. van (2003). *The Analysis of Polymer Interfaces, a Combined Approach*, chapt 7, Universiteitsdrukkerij Technische Universiteit Eindhoven, Eindhoven, NL, 89.
[13] Kjellander, B. K. C., van Ijzendoorn, L. J., de Jong, A. M., Broer, D. J., van Gennip, W. J. H., de Voigt, M. J. A., & Niemantsverdriet, H. J. W., (2004). *SPIE-IS&T Proc.*, 2589, 94.
[14] Manly, B. J. F. (1986). *Multivariate Statistical Methods, a Primer*, Chapman and Hall: Bristol, UK.
[15] Maisel, L. (1971). *Probability, Statistics and Random Processes*, Simon & Schuster: New York, 275.